

SEP Temporal Fluctuations Related to Extreme Solar Flare Events Detected by SOHO/CELIAS/SEM

Leonid V Didkovsky, Darrell L Judge, Seth Wieman, Andrew R. Jones,
Pradip Gangopadhyay, Matt Harmon,*
University of Southern California, Los Angeles, CA, 90089, USA

W Kent Tobiska †
Space Environment Technologies, Pacific Palisades, CA 90272, USA

The SOHO CELIAS/SEM measurements of the solar Extreme Ultraviolet (EUV) irradiance in the He II 30.4 nm first-order channel (26–34 nm) are highly sensitive to impacts of Solar Energetic Particles (SEP). A model of the SEM response to a quasi-isotropic SEP fluence allowed us to determine both the range of proton incident energies and the SEM sensitivity to the SEP flux, which has a maximum around 12 MeV. We propose to use high-cadence (15 s) SEM first-order count-rates to analyze the temporal fluctuations of the SEP flux arriving from extreme solar flare events. A comparison of these temporal fluctuations for the July 14, 2000, October 28, November 2, November 4, 2003, and January 20, 2005 events shows that the most intense high-frequency RMS variations of the first-order count-rates at the time when SEPs started to arrive, were associated with the January 20 event. These high-frequency variations are produced by packets of SEPs. Two (plus and minus) first-order SEM detectors with the distance between them of about 62 mm allow us to analyze the spatial coincidences and temporal distribution of SEP related signals at 1 AU. The largest temporal separation of the SEP packets is observed at the time when the packets start to arrive. RMS fluctuations (variances) for all analyzed events do not follow the photon noise (\sqrt{N}) in assumption of the Poisson or normal distribution but correlate ($R = 0.999$) with the speed at which the SEP flux grows. If the found correlation is confirmed on a larger statistical data base, it may allow the prediction of the SEP flux growth profile by analyzing the RMS amplitudes for the initial phase of the SEP impact.

Nomenclature

CR Count rate, 1/s
 E SEP energy, MeV
 R SEM response, e/particle

I. Introduction

Extreme solar flare events, usually associated with the largest X-class solar flares, are the most interesting events from the point of view of studying their energy release in a wide spectrum of solar radiation and their impact on the Earth's environment. The energy associated with solar flares is released in the forms of electro-magnetic radiation and accelerated particles. Solar flares are responsible for an initial acceleration of the particles and for creating some post-flare conditions, like Coronal Mass Ejection (CME) driven shock waves for the further acceleration of the Solar Energetic Particles (SEP) to energies of hundreds or thousands of MeV. The great interest in studying SEPs arises from the fact that they give us information required to verify the models of the acceleration mechanisms. There are a few approaches to studying SEPs. One of them is based on determining the flare specific chemical composition of the ejected ions, and their energies and fluxes by, for example, using Advanced Composition Explorer (ACE) data.^{1,2} Another way is to study

SEPs in a number of relatively narrow incident energy ranges, e.g., with the energetic particle instrument SOHO/ERNE,³ which covers the energy range from 1.3 MeV nucl^{-1} to about 110 MeV nucl^{-1} for protons and alpha particles. Protons with higher energies and wider energy ranges, e.g., 165 – 500 MeV are observed by GOES. We have developed a method⁴ of extracting high-energy proton fluxes (up to about 400 MeV) with energy ranges narrower than GOES using SOHO/EIT CCD corner areas outside the solar disk images.

The SOHO CELIAS/SEM instrument⁵ for measuring solar Extreme Ultraviolet (EUV) solar irradiance has never been used to detect the SEPs. However, the first-order channel of the SEM, which measures solar EUV flux in the 26 – 34 nm spectral range is sensitive to SEPs and its count-rate signal includes a component produced by SEP flux during extreme solar flare events. The great advantage of using this channel for extracting SEP information is its high (15 s) cadence. An opto-mechanical model of the SEM shows the SEM response to the high-energy particles and determines the SEP energy range where the first order channel is the most sensitive to the particles. We have used the sensitivity of this SEM channel, as determined by the model, to better compare the SEP related fluctuations extracted from SEM with the rising phases of the GOES proton fluxes in the energy range of 8 – 16 MeV.

II. Modeled sensitivity of the SEM to quasi-isotropic SEP fluence

A model of the SEM response to the SEP fluence is based on a geometrically accurate 3-dimensional representation of all SEMs components including its envelope, and was generated using SolidWorks mechanical design software. The position of the SEM on the SOHO platform was also considered for modeling back-side SEP trajectories. In the model, straight-line proton trajectories through the detector are considered for a series of different approach angles. For each of these paths, the amount of material traversed by the proton as it passes through the SEM envelope and other ancillary structures en route to the detector is determined, as is the proton path length through the detector itself. These path lengths, along with the proton stopping powers of the materials encountered, are used in determining the reduced energy, E_r , which the proton retains when it reaches the detector and, ultimately, the energy it deposits in the detector (proportional to detector response).

$$E_r(\Theta, \Phi) = E_i(\Theta, \Phi) - E_s(\Theta, \Phi), \quad (1)$$

where $E_i(\Theta, \Phi)$ and $E_s(\Theta, \Phi)$ are the proton incident energy and the stopping power, respectively. The mean SEM response to protons of a given energy of interest, $\mathcal{R}(E)$, averaged over a specified range of incidence angles on a spherical coordinate system with origin at the center of the active region of the detector, and with azimuth Θ and polar angle Φ , is given by:

$$\mathcal{R}(E) = \frac{\int_{\Theta_1}^{\Theta_2} \int_{\Phi_1}^{\Phi_2} R(E, \Theta, \Phi) \cdot \sin\Phi \cdot d\Theta \cdot d\Phi}{\int_{\Theta_1}^{\Theta_2} \int_{\Phi_1}^{\Phi_2} \sin\Phi \cdot d\Theta \cdot d\Phi}, \quad (2)$$

where the $R(E, \Theta, \Phi)$ is an individual SEM response for each of 360,000 test directions. Here

$$R(E, \Theta, \Phi) = \frac{E_r(\Theta, \Phi)}{E_{ion}}, \quad (3)$$

where $E_{ion} = 3.65 \text{ e/eV}$ is the energy of ionization of the silicon.

Alternatively to the global integration over the sphere, the mean response $\mathcal{R}(E)$ can be obtained by averaging the response for N different trajectories selected randomly over the angle range of interest. For sufficiently large N, this method gives virtually identical results to the numerical evaluation of Eq. (2). Fig 1 shows the average first-order SEM response as a function of initial proton energy for three different angle ranges.

Fig 1 indicates a maximum SEM response to protons at about 12 MeV. The response function is highly sensitive to the incident angle. The thick line shows the response averaged for incidence angles ranging over a full sphere (4π steradian) solid angle. The lower dotted line shows the response for incidence angles confined to a ± 60 deg cone (1π sr) about an axis normal to the detector (parallel to the instrument optical axis). Averaging over a ± 60 deg cone about an axis parallel to the detector surface, as shown by the upper dashed line, indicates that the SEM is more sensitive to grazing incidence SEPs, which trace a much longer path through the detector active region depositing greater energy. As the peak of the response function remains close to 12 MeV irrespective of incidence angle, we have assumed GOES data in an energy range of

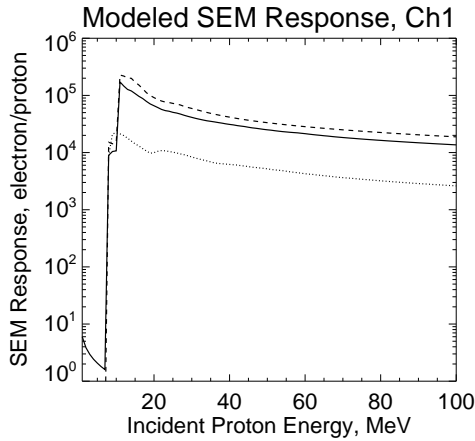


Figure 1. Average SEM response to three different SEP fluences. Thick line shows quasi-isotropic response averaged for incidence angles ranging over a full sphere (4π steradians) solid angle. The lower dotted line and upper dashed line show the average response for incidence angles confined to a ± 60 deg cone about the detector normal and about an axis parallel to the detector surface respectively.

8 – 16 MeV to be a logical reference proton flux with which to compare the rising SEP count-rate detected by the first-order SEM channel. Fig 1 also shows that protons with energies lower than about 10 MeV are stopped by the SEM envelope and do not reach the SEM detector. The exact amount of the first-order SEM signal created by SEPs is not the subject of this paper. We will compare SEM and GOES profiles just to determine how well the time of increased fluctuations in the first-order count-rates matches the arrival time measured using the GOES proton flux profile.

III. Data Observations and Analysis

For this paper we have analyzed five extreme solar flare events, Bastille Day (BD) of July 14, 2000, three Halloween (2003) events of October 28, November 2 and 4, and one of the most intense and the largest ground-level events (GLE) since 1956,⁶ the January 20, 2005 event. The October 28, 2003 event showed about 5 times larger ionospheric impact in the measured Total Electron Content (TEC) than the BD and Halloween events.⁷ Each of these five days consists of about 5760 SEM measurements with 15-s cadence.

A. Using a mean signal from the plus and minus first-order channels

The SEM has two (plus and minus) first order “30.4 nm” channels. The EUV measurements in these first-order channels were affected (after the EUV peak of the flare) by the extreme solar flare events and the resulting signal in each channel consists a sum of count-rates produced by the photon flux in the 26 – 34 nm wavelength range and the SEP flux. The EUV responses in both first order channels are quite close to each other and are usually represented by a mean first-order signal for most scientific applications. We have started our analysis of the SEP related fluctuations with the mean count-rate \mathcal{A}_1 from the first-order measurements. To separate the higher frequency fluctuations of the signal from a lower frequency trend we used a running mean curve A_{RM} with a temporal window of 7 – 27 15 s points, equal to 1.75 – 6.75 min integration. The fluctuations then were determined as residuals A_{RES} after subtracting the running mean curve from the measurements.

$$A_{RES}(t) = \mathcal{A}_1(t) - A_{RM}(t) \quad (4)$$

The EUV part of the residual signal either does not show any short period (e.g., less than 1 min) *regular* flare related fluctuations or the amplitude of these fluctuations is quite low in this temporal domain. In contrast, the SEP related part of the residual signal begins to show some fluctuations at the time when the SEPs started to arrive. This allowed us to assume that the main portion of the residual signal in the form of regular high-frequency fluctuations is related to the SEP impact. These SEP related fluctuations are packets of particles arrived to the detectors at the same 15 s integration time as a combination of individual particle

events, e.g. with different energies, trajectories, and initiation times.

B. Comparing residuals taken separately from the first-order channels

At the next stage of the analysis we extracted the residual signals separately from each plus and minus first order channel. The extracting procedure was exactly the same as described by Eq. (4) with the results for each channel stored separately. The next step in the analysis was comparing the residuals for the two separate channels. The data sets were divided in two parts for each analyzed event, before the time when SEPs started to arrive, and after that time. To decrease the influence of a difference in the channel responses to EUV flux, which was dominant in the first parts of the residuals, we have excluded low amplitude (less than 0.55 counts/s) fluctuations and then calculated cross-correlations between the plus and minus channel residuals. The cross-correlation coefficients for the first 'flare' parts of the data (not affected by the particle signal) with the short temporal window of seven 15-s intervals are in a range of 0.6 – 0.8, while the cross-correlation for the second 'SEP' parts is low and varies from 0.05 to 0.26 for different events and periods of determining the SEP flux. Choosing a larger running mean window, e.g., 27 or 57 points improves the correlation between the 'flare' residuals to 0.90 – 0.97 with about the same low correlation for the 'SEP' parts. These correlated vs. uncorrelated fluctuations represent the difference between the photon and particle fluxes. The much larger photon flux during the initial phase of the flare forms a wave with a common wavefront while the particles, which arrive later, are unsynchronized at the detectors.

IV. Results

One of the goals of this analysis was to find out if the amplitude of SEP related short-time fluctuations follow the photon noise statistics (\sqrt{N}), where N is a number of particles coming to the detector. In other words, to find out whether the SEP fluctuations in the form of count-rate peaks have a statistical noise pattern determined by the SEP flux, i.e. do larger fluctuations correspond to larger flux, or are they independent of flux intensity, but related to SEP initiation and acceleration. The residual fluctuations related to the SEP flux were analyzed for five extreme solar flare events. We have found that for all of these events the SEP fluctuations start as some discrete packets of peaks. The residuals A_{RES} Eq. (2) have zero amplitude when the measured SEM signal is equal to the running mean signal, which occurs when the measurements contain just low frequency variations ($1/60T$ and lower, where T is the SEM sampling interval equal to 15 sec) not analyzed in this work. We have analyzed higher frequency fluctuations in the range of $1/2T$ to $1/60T \text{ s}^{-1}$. The residual fluctuations were first extracted from the mean first-order channel and then separately from both (plus and minus) first-order channels.

A. Residuals from the mean first-order signal

Figure 2 shows examples for the October 28, 2003 and January 20, 2005 events. The residuals from the mean first-order channel are plotted for the time when the SEPs started to arrive.

Figure 2 shows initial periods of SEP detection. When the arriving SEP flux is low and growing, the detected fluctuations do not overlap each other and form a few easily distinguished groups or packets related to both particle distribution and acceleration mechanism. Zero signal residuals appear more often and are longer between any two groups of fluctuations at the beginning of the SEP impact than when the SEP flux becomes more intense. As the SEP flux grows, the zero flux time intervals become shorter, or are totally overlapping and finally the fluctuations can be seen as one large group. Thus, the SEP packets show larger temporal separation for the initial phases of the SEP impacts. These fluctuations represent changes in the SEP flux, which occur when the number of particles that reach the detector is varying about the mean level. Groups of particles may represent isolated events or, may be created when particles that reach the detector at 1 AU are combined with those ejected later but accelerated to a higher speed or with those ejected earlier but having a lower speed. Alternatively, the group may be created combining different trajectories along the Interplanetary Magnetic Field (IMF) lines or different pitch angles. The features in the distribution of the peaks extracted for this initial phase of SEP events (amplitude and shape of the fluctuation peak) may be used either to model the particle production and acceleration mechanisms or to verify the existing acceleration models.

As the packets with about the same amplitudes are present at the time when the SEP flux begins and when it reaches its maximum values, we can assume that the high-frequency fluctuations represent groups

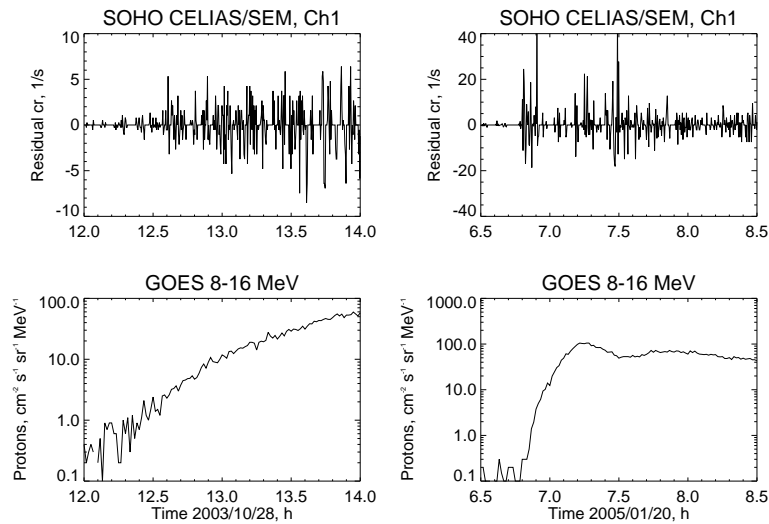


Figure 2. Left. SEM residual count-rate fluctuations (top) and GOES proton flux in 8 – 16 MeV (bottom) for the Oct. 28, 2003 event. Right. The same for the Jan. 20, 2005 event. Note that the intense SEM fluctuations (top) begin at the same time as GOES shows increase in the proton flux. Much smaller GOES flux fluctuations are related to the four time larger (1 min) GOES integration time.

of particles compressed in time and distance rather than signal changes associated with individual particles. Because the SEP flux in the energy range of SEM sensitivity (about 12 MeV) is changed more than two orders of magnitude from the beginning of the extreme event to its maximum, the relative impact on the 30.4 nm channel signals from individual particles is decreased accordingly. Figure 2 (right) shows the case when initial fluctuations (e.g., around 6.9 h) with the low SEP flux have larger amplitudes than the fluctuations at about 7.1 h when the SEP flux is 2 orders of magnitude larger. If the fluctuations show just a statistical photon noise (\sqrt{N}), then the relative amplitude of the fluctuations would strongly depend on the SEP flux, increasing with increasing flux, while in fact we see (Figure 2) that this is not the case.

Figure 2 shows that the amplitude of the SEP fluctuations at the time when the SEP flux grows from 1 to 10 flux units is not the function of SEP flux intensity. We have found that for the initial phase of SEP flux the amplitude of fluctuation peaks is correlated with the temporal Growth Rate (GR) of the particle flux. The statistics of this correlation are not sufficient with the five analyzed events to draw more than suggestive or tentative conclusions. Nevertheless, this feature may be explained if we assume that the number of particles that create a fluctuation peak is directly related to the probability of their being combined with other particles created at (about) the same time. This probability depends on the speed of the rising phase and may be measured by the SEP profile GR (see also Table 1) or by the first derivative of the flux rising profile. Figure 3 illustrates this correlation, which is 0.999.

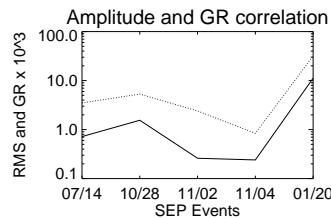


Figure 3. SEM residual RMS amplitude (solid line) and the temporal growth rate (GR) changes (dotted line) for the analyzed events. Both RMS amplitudes and GR were calculated for the same time interval of 10 min after SEPs started to arrive to the SEM detector.

We have combined the main characteristics of the SEP related fluctuations in the first-order SEM signal in Table 1. Table 1 shows the time of SEP arrival, RMS values (for 40 time intervals each) determined for the

analyzed events, *before* the moment of the SEP impact (RMS_1), and *afterwards*, (RMS_2), and the growth rate (dF/dT) of the SEP flux growth profile determined for the same 40 time intervals ($dT = 600$ s).

Table 1. Some characteristics of the SEP related fluctuations in the SEM first-order channel

Date	SEP Time, h	RMS_1 , 1/s	RMS_2 , 1/s	dF/dT , $1/(\text{cm}^2 \text{ sr MeV s}^2)$
2000/07/14	10.90	0.08	0.72	$3.5e^{-3}$
2003/10/28	12.55	0.53	1.55	$5.3e^{-3}$
2003/11/02	17.68	0.13	0.26	$2.4e^{-3}$
2003/11/04	22.17	0.21	0.24	$8.4e^{-4}$
2005/01/20	6.80	0.47	11.20	$3.2e^{-2}$

Table 1 represents the increase of the RMS fluctuations after the beginning of the arrival of SEPs. The maximal increase with about 6 times larger growth rate ($\text{GR} = dF/dT$) than for the most powerful 'ionospheric' event of October 28, 2003⁷ was detected for the January 20, 2005 event. The minimal increase of RMS_2 for the November 4 event is caused by a relatively low SEP flux due to the limb position of the solar flare. The growth of the SEP flux was just about 2 particles per ($\text{cm}^2 \text{ sr MeV s}$) during the two hours after the event had started. To compare, the November 2 event showed three times larger growth of the SEP flux 0.3 hours after the event had started.

B. Residuals from separated first-order signals

The pre-flight calibration of the SEM instrument with an EUV source of irradiation, and real solar EUV measurements during sounding rocket flights, as well as onboard SOHO measurements showed very similar changes of the EUV related signals in both first-order channels. Similarly, the SEP contribution to the first-order count-rates, produced by an intense SEP flux, reflect *macro* changes of the SEP flux and are, of course, highly correlated to each other. In contrast to the macro changes of the signals, the *residuals* from these channels represent short time fluctuations around the running mean and reflect the statistical distribution of the photons and/or particles on two separated detectors during each 15 s integration time.

In the case of residuals, the statistics of coincidences depends on a few factors. First of all, it reflects the number and intensity of EUV signal fluctuations. Practically all EUV changes with a significant amplitude (e.g. more than 0.5 counts/s) nominally show good coincidence peaks. Moreover, the correlation of these peaks becomes higher if the EUV changes are longer than one 15 s interval (they usually are), and a wider running mean window is applied to extract the residuals.

Secondly, the frequency of coincidences depends on the SEP flux intensity in the range of SEM channel sensitivity. The higher the SEP flux, the more frequent the coincidences. In contrast to the EUV example, in the case of SEP related fluctuations the correlation in the first-order channels drops as longer running mean windows (lower frequencies) are used.

Thirdly, there is a non-zero probability of some type of SEP quasi waves when particles form flat front waves similar to photons. Following some acceleration conditions they may form a number of SEP 'clouds' of particles with a quasi synchronous impact on two separate but closely located detectors. A SEP event detected at 1 AU after the extreme solar flare is a type of big and long lasting particle 'cloud', which may develop a 'fine structure' when analyzed with the 15 s SEM cadence. Obviously, this 'fine structure' is easier to detect at the beginning of an event when the number of overlapping 'clouds' is small, the analysis of which we have proposed in this work.

The different dependence of the EUV and SEP coincidences on the time intervals selected for signal averaging may be used for separating (refining) of these residual fluctuations. To identify the EUV part we have to find, in general, coincidences of more than one 15 s interval, and form from these long lived coincidence peaks the EUV contribution to the fluctuations. To refine the SEP related signal we have to subtract these long lived EUV coincidence data from the composite residual fluctuations.

The whole refining procedure consists of the following steps. First, the residuals from the plus and minus first-order channels (Eq. 4) were extracted and compared using a logical AND coincidence technique

$$Ch_{1\&2}(t) = (Ch1(t) + Ch2(t))/2 \mid (Ch1(t)\&\&Ch2(t)) > 0.0 \quad (5)$$

or

$$Ch_{1\&2}(t) = (Ch1(t) + Ch2(t))/2 \mid (Ch1(t)\&\&Ch2(t)) < 0.0 \quad (6)$$

where \mid and $\&\&$ means IF and AND, respectively. After that, we have compared the coincidence residuals for two sizes of the running mean window, one for 7 high cadence (15 s data) points (1.75 min), and another for 27 points (6.75 min). Figure 4 (top and middle panels) shows the result. As expected, the important difference between the coincidence signals 1 & 2 (top and middle panels on Fig. 3) is some peak shape changes. Some peaks have increased both in time span and their amplitude when the running mean window was changed from 7 to 27 points. These peaks match each other qualitatively better in all three plots in middle panel than in the top panel, e.g., note the peaks at about 12.64 h. We assume that the major portion of these wide coincidence signals (structures), wider than one 15 s time interval, are due the EUV signal fluctuations. Other peaks, unchanged and short in amplitude and time duration, represent the SEP related fluctuations.

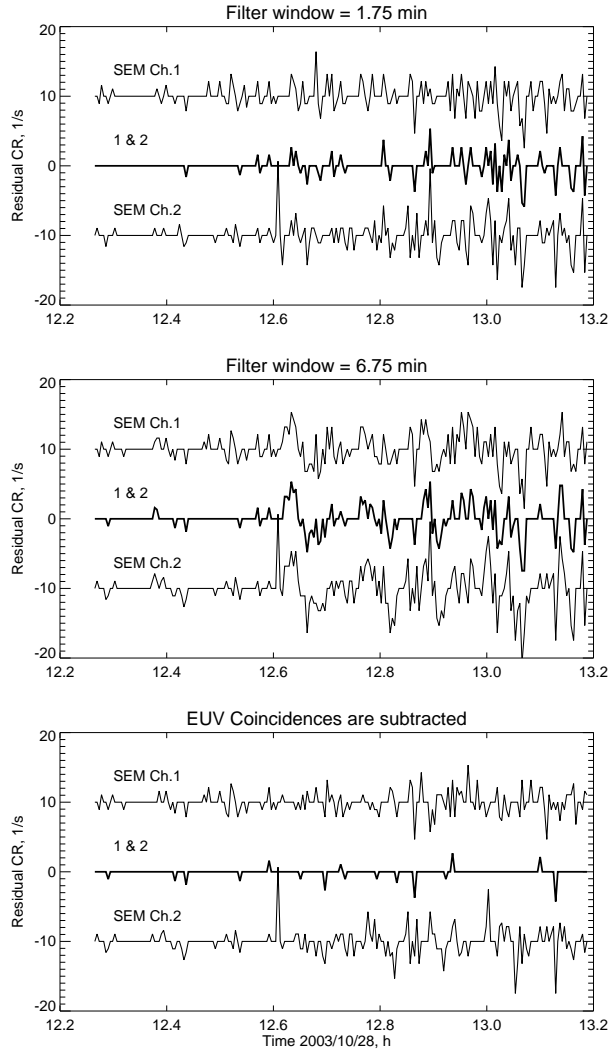


Figure 4. SEM residual count-rate fluctuations extracted from the plus first-order channel (Ch. 1) and the minus channel (Ch. 2) together with their coincidence fluctuations (1 & 2). The top and middle plots show two types of temporal filtering, by using a running mean with windows of 1.75 and 6.75 min, respectively. The signals of Ch. 1 and Ch. 2 are shifted by ± 10 units for clarity of viewing the data. The bottom panel shows a refined time series of the SEP related coincidence fluctuations (thick line) using a temporal filter with a window of 6.75 min.

Finally, these wider coincidence peaks were subtracted from the Ch. 1 and Ch. 2 (Fig 4, bottom panel)

for refining the SEP related signals.

$$Ch_{SEP1}(t) = Ch1(t) - Ch_{1\&2}(t) \mid (Ch_{1\&2}(t-1) = 0.0 \&\& Ch_{1\&2}(t) \neq 0.0 \&\& Ch_{1\&2}(t+1) \neq 0.0 \quad (7)$$

and

$$Ch_{SEP2}(t) = Ch2(t) - Ch_{1\&2}(t) \mid (Ch_{1\&2}(t-1) = 0.0 \&\& Ch_{1\&2}(t) \neq 0.0 \&\& Ch_{1\&2}(t+1) \neq 0.0 \quad (8)$$

$$Ch_{SEP1\&2}(t) = 0.0 \mid (Ch_{1\&2}(t-1) = 0.0 \&\& Ch_{1\&2}(t) \neq 0.0 \&\& Ch_{1\&2}(t+1) \neq 0.0 \quad (9)$$

or

$$Ch_{SEP1\&2}(t) = Ch_{1\&2}(t) \mid (Ch_{1\&2}(t-1) = 0.0 \&\& Ch_{1\&2}(t) \neq 0.0 \&\& Ch_{1\&2}(t+1) = 0.0 \quad (10)$$

The bottom panel shows a new coincidence sequence 1 & 2 (thick line), where only one time interval (15 s) points are present.

V. Concluding comments

The short time (15 s) fluctuations extracted from the SOHO/SEM first-order channels show clear evidence of SEP related peaks during severe X-ray storms. Our SEM proton sensitivity model showed that SEM EUV measurements could be contaminated by SEP flux with proton incident energies above 10 MeV, with the sensitivity peak around 12 MeV for quasi-isotropic particle fluence. More spatially concentrated SEP beams do not change the position of the sensitivity peak but change the response function.

The present analysis of high-cadence fluctuations in the residual SOHO/SEM first-order channel count-rates allows us to extract information about the distribution of the SEP related packets of particles. The packets are clearly separated from each other at the onset of SEP impact. RMS amplitudes of these SEP related peaks reflect the flare and post-flare SEP dynamics and are different for the analyzed events, showing that the maximal RMS amplitude occurs for the January 20, 2005 event. The RMS amplitudes of the residual peaks do not show the (\sqrt{N}) dependence and are related to the speed of the SEP growth phase and may be estimated using a Growth Rate (GR) parameter. We have found a high correlation (0.999) between the changes of the RMS amplitude and the GRs for all five analyzed events, but additional statistics are required to establish this correlation.

The SEP separation intervals, together with the amplitudes of the residual peaks have been used to identify a sequence of events from the plus and minus first-order channel data. The coincidence peaks extracted from these data contain both EUV and SEP contributions and have been separated (refined) by assuming that all wide coincidence peaks are related to the EUV part of the SEM signal. Even with this possible underestimation of the SEP related coincidences in the two first-order channels, the information about these fluctuations may be used to model the SEP acceleration and dynamics.

Acknowledgments

This work was supported in part by the NASA Grant NNG 05WC09G.

References

- ¹Stone, E.C., Frandsen, A.M., Newaldt, R.A., Christian, E.R., Margolies, D., Ormes, J.F., Snow, F., The Advanced Composition Explorer, *Space Science Reviews*, Vol 86, pp.1, 1998.
- ²Stone, E.C., Burlaga, L.F., Cummings, A.C., Feldman, W.C., Frain, W.E., Geiss, G., Gloeckler, G., Gold, R., Hovestadt, D. et al., The Advanced Composition Explorer, Particle Astrophysics *AIP Conf Proc*, Vol 203, pp.48, 1998.
- ³Torsti, J., Valtonen, E., Lumme, M., Peltonen, P., Eronen, T., Louhola, M., Riihonen, E., Schultz, G., Teittinen, et al., *Solar Phys.*, 162, pp. 505, 1995.
- ⁴Didkovsky, L.V., Judge, D.L., Jones, A.R., Rhodes, E.J., Jr., Gurman, J.B., Measuring proton energies and fluxes using EIT (SOHO) CCD areas outside the solar disk images, *Astron. Nachr / AN*, 327, No.4, pp. 314, 2006.
- ⁵Judge, D.L., McMullin, D.R., Ogawa, H.S. et al., First Solar EUV Irradiance obtained from SOHO by the CELIAS/SEM, *Solar Phys.*, 177, pp. 161, 1998.
- ⁶Bieber, J.W., Clem, J., Evenson, P., Pyle, R., Duldig, M., Humble, J., Ruffolo, D., Rujiwarodom, M., Saiz, A., Largest GLE in Half a Century: Neutron Monitor Observations of the January 20, 2005 Event, *29th International Cosmic Ray Conf.*, 1, pp. 237, 2005.

⁷Tsurutani, B.T., Judge, D.L., Guarnieri, F.L., Gangopadhyay, P., Jones, A.R., Nuttall, J., Zambon, G.A., Didkovsky, L., A.J. Mannucci, B. Iijima, R. R. Meier, T.J. Immel, , T. N. Woods, S. Prasad , J. Huba, S. C. Solomon, P. Straus, R. Viereck, The October 28, 2003 extreme EUV solar flare and resultant extreme ionospheric effect: Comparison to other Halloween events and the Bastille Day event, *GRL*, 32, L03S09, 2005.